ISSN 1063-7826, Semiconductors, 2014, Vol. 48, No. 10, pp. 1303–1307. © Pleiades Publishing, Ltd., 2014.
Original Russian Text © I.E. Tyschenko, V.A. Volodin, V.V. Kozlovski, V.P. Popov, 2014, published in Fizika i Tekhnika Poluprovodnikov, 2014, Vol. 48, No. 10, pp. 1339–1343.

SURFACES, INTERFACES, AND THIN FILMS

Effect of Hydrostatic Pressure during the Annealing of Silicon-on-Insulator Films Implanted with a High Hydrogen-Ion Dose

I. E. Tyschenko[a,^], V. A. Volodin[a,b], V. V. Kozlovski[c], and V. P. Popov[a]

[a] *Rzhanov Institute of Semiconductor Physics, Siberian Branch, Russian Academy of Sciences, pr. Akad. Lavrent'eva 13, Novosibirsk, 630090 Russia*

^ *e-mail: tys@isp.nsc.ru*

[b] *Novosibirsk State University, ul. Pirogova 2, Novosibirsk, 630090 Russia*

[c] *St Petersburg State Polytechnical University, ul. Polytekhnicheskaya 29, St. Petersburg, 194251 Russia*

Submitted March 20, 2014; accepted for publication April 28, 2014

Abstract—The properties of silicon-on-insulator films implanted with high hydrogen-ion doses (~50 at %) and annealed under a pressure of 10.5 kbar are studied using the Raman scattering (RS) method. A high degree of optical-phonon localization is detected in the films under study, which is retained to an annealing temperature of ~1000°C and is explained by the formation of silicon nanocrystals. It is found that the activation energy of annealing of the structural relaxation of dangling bonds in films with a high hydrogen content is independent of the annealing pressure. The activation energy of growth of the crystalline phase, calculated from RS spectra is ~1.5 eV and is independent of pressure. The effect of hydrostatic pressure consists only in a decrease in the frequency factor limiting Si–Si bond relaxation during ordering.

DOI: 10.1134/S1063782614100285

1. INTRODUCTION

Nanocrystalline silicon consisting of nanocrystals spaced by an amorphous interlayer is attracting the significant attention of researchers as a material promising from the viewpoint of the development of highly efficient thin-film solar cells [1, 2]. In comparison with low-cost amorphous silicon, nanocrystalline silicon films are highly stable to sunlight and have a long carrier lifetime and a wide spectral range of light absorption. The properties of such a material depend on its structure, in particular, on the content and sizes of nanocrystalline grains and on the state of the interface between the grain and surrounding amorphous matrix [3]. In [4–6], it was shown that the implantation of high hydrogen-ion doses into thin silicon films is accompanied by the formation of nanocrystalline silicon. In this case, the sizes of the nanocrystals and their volume fraction depend on the concentration of implanted hydrogen atoms and subsequent annealing temperature and duration.

There are published data that the behavior of hydrogen implanted into silicon depends on external pressure. According to the published data, the critical radius of hydrogen-bubble formation should increase with external pressure [7]. In other words, an increase in the external pressure inhibits hydrogen-solid-solution layering in silicon. It is this effect that was identified as the cause of the formation of a thin surface hydrogen-containing silicon layer upon the annealing of silicon films implanted with hydrogen ions under pressure[8]. In [9], quantum-chemical calculations of hydrogen diffusion in silicon and germanium were performed, on the basis of which it was concluded that the pressure causes hydrogen-diffusion deceleration in silicon due to the increasing potential barrier for hydrogen-atom escape from the bound state. This means that annealing under high pressure can inhibit the crystallization of silicon films with a high hydrogen content. The objective of this work is to study the structural properties of silicon-on-insulator (SOI) thin films implanted with high doses of hydrogen ions and annealed under high hydrostatic compression.

2. EXPERIMENTAL

The study was conducted on SOI (100) structures whose fabrication method was described in [5, 6]. The thickness of the cut silicon layer was 280 nm, and the buried SiO_2 thickness was ~400 nm. Implantation was performed with hydrogen ions from a plasma pulsed source with an energy of 24 keV and a dose of 5×10^{17} cm^{-2} under conditions providing near-room sample temperature. The used implantation parameters provided a hydrogen concentration of 50 at % in the silicon film. Subsequent annealing of the implanted structures was performed in a high-pressure furnace at a temperature of 450–1000°C for 1 h in an argon atmosphere under hydrostatic compression of 10.5 kbar. The structures were analyzed by Raman

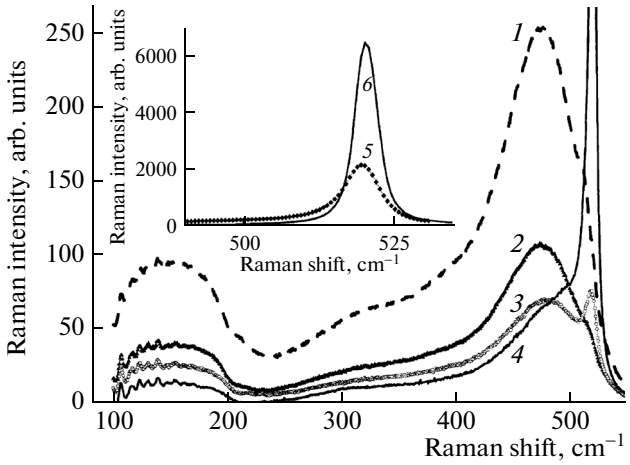

Fig. 1. RS spectra of SOI films implanted with hydrogen ions with an energy of 24 keV and a dose of 5×10^{17} cm^{-2} (*1*) before and after annealing at temperatures of (*2*) 450, (*3*) 600, (*4*) 800, and (*5*, *6*) 1100°C under pressures of (*2–5*) 10.5 kbar and (*6*) 1 bar.

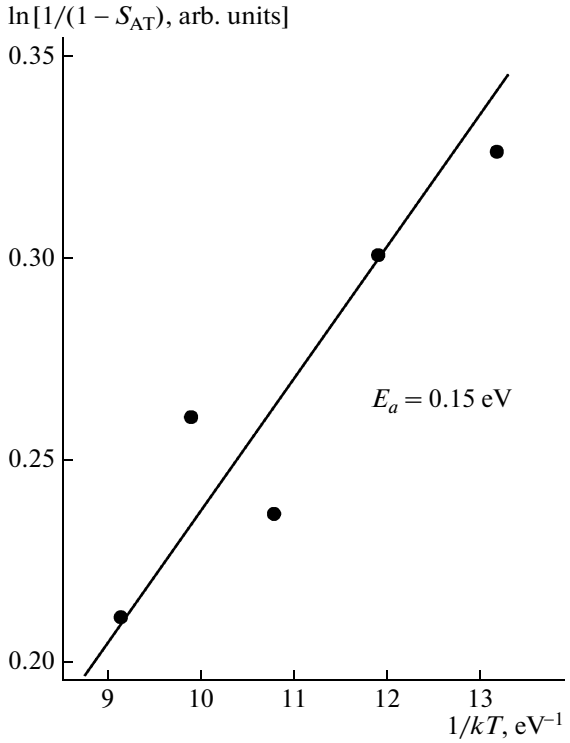

Fig. 2. Logarithmic variation in the relative RS peak area with a maximum at ~150 cm^{-1} as a function of the inverse temperature of annealing under a pressure of 10.5 kbar of SOI films implanted with hydrogen ions with an energy of 24 keV and a dose of 5×10^{17} cm^{-2}.

scattering (RS) spectroscopy. The RS spectra were excited by an Ar-laser line with a wavelength of 514.5 nm, with a sample-reaching power of 2–3 mW recorded at room temperature. The probing spot size was 4–6 μm. A spectrometer with a T64000 triple monochromator (Horiba Jobin Yvon) with a spectral resolution no worse than 2 cm^{-1} was used. A silicon matrix of photodetectors cooled by liquid nitrogen was the detector. Measurements were performed in the backscattering geometry with the polarization vector of incident radiation directed along the ⟨011⟩ silicon crystallographic direction. Scattered light was measured in the $\langle 01\bar{1} \rangle$ polarization. The chosen geometry allowed the maximum suppression of the RS signal of the silicon substrate.

3. RESULTS AND DISCUSSION

Figure 1 shows the RS spectra of SOI films implanted with hydrogen ions before and after annealing at temperatures of 450, 600, 800, and 1000°C under a pressure of 10.5 kbar (curves *2–5*) and 1 bar (curve *6*). In the RS spectra of the unannealed samples, several bands were observed, whose intensity and energy position vary with increasing temperature of subsequent annealing. In the low-frequency spectral range of 100–200 cm^{-1}, broad band is observed whose frequency position corresponds to the frequency of the transverse acoustic phonon at the Brillouin-zone boundary of the silicon lattice. In single-crystal silicon, this peak is invisible due to the selection rules forbidding light scattering at phonons with larger momenta. Defect generation in the implanted films violates the crystal translational symmetry and results in scattering ban removal in this spectral range. Annealing of the implanted layers causes radiation-defect recombination and crystal-structure restoration, which is accompanied by reduced scattering at long-wavelength oscillations. We can see in Fig. 1 that annealing under pressure is accompanied by a monotonic decrease in the scattering intensity at the acoustic phonon frequency in the entire temperature range. Analysis of the logarithmic dependence of the variation in the relative area of the RS peak with a maximum at ~150 cm^{-1} on the inverse temperature of annealing under a pressure of 10.5 kbar is shown in Fig. 2. We can see that the behavior of the low-frequency RS peak area variation is approximated in the entire temperature range by a straight line with a slope corresponding to an activation energy of 0.15 ± 0.02 eV. This value is close to the activation energy of the structural relaxation of dangling bonds in hydrogenated amorphous silicon [10, 11]. This suggests that structural-disorder annealing in silicon films implanted with high hydrogen-ion doses under conditions of hydrostatic compression is identical to defect annealing at atmospheric pressure [6].

In the region of the frequency of 300 cm^{-1}, a scattering shoulder is observed, which can be caused by scattering at longitudinal acoustic and optical modes in silicon (Fig. 1). The intensity of this scattering also decreases with increasing annealing temperature.

In the frequency range of optical phonons, a broad peak with a maximum at 473 cm^{-1} is observed immediately after hydrogen-ion implantation. Its position corresponds to the frequency of the transverse optical phonon in hydrogenated amorphous silicon [12]. As the annealing temperature increases, the energy position of this peak shifts to the high-frequency region; after annealing at 800°C, it reaches a position of 480 cm^{-1} corresponding to the frequency of the optical phonon localized in disordered silicon. The peak intensity decreases with temperature and almost disappears at 1000°C.

In addition to the broad RS peak at Si–Si vibrations in the amorphous phase, asymmetry shaped as a weakly expressed shoulder in the long-wavelength region is observed in the RS spectrum of the unannealed films. After expanding the broad peak into Gaussian components, a peak with a maximum at 513.4 cm^{-1} was distinguished, whose full width at half maximum (FWHM) is 10.1 cm^{-1}. After annealing at a temperature of 450°C under a pressure of 10.5 kbar, this shoulder is transformed into a more distinct peak with a maximum at 517.4 cm^{-1}. As the annealing temperature increases, its position shifts to the low-frequency region, reaching 519.5 cm^{-1} after 700°C. A further increase in the annealing temperature does not affect the energy position of this peak, but is only accompanied by an increase in its intensity. The nature of this peak is associated with scattering at the frequency of the transverse optical phonon localized in the nanoscale silicon volume [13]. Figure 3 shows the position of the optical-phonon frequency (curves *1* and *2*) and the scattering-band broadening relative to the width in single-crystal silicon (curves *3* and *4*) as functions of the annealing temperature at atmospheric pressure [6] and a pressure of 10.5 kbar. We can see that an increase in the pressure during annealing by a factor of 10^4 result in, first, a low-energy frequency shift of the optical phonon; second, corresponding RS-line broadening. The RS-peak width after annealing at 1000°C remains about 7 cm^{-1} which is almost two times larger than in single-crystal silicon. At the same time, the peak intensity is three times lower than that for films annealed at atmospheric pressure. This means that the fraction of the crystalline phase after annealing under high pressure is less than after annealing under atmospheric conditions. The low-frequency shift in the optical-phonon peak position can be caused, on the one hand, by the presence of the nanocrystalline volume; on the other hand, by the presence of stresses caused by structural defects.

Quantitative analysis of the RS spectra allows determination of the volume fraction of the crystalline phase using the expression $\rho_c = I_c/(I_c + yI_a)$, in which I_c and I_a are the corresponding total RS intensities in the crystalline and amorphous phases; $y = \Sigma_c/\Sigma_a$, where Σ_c and Σ_a are the total backscattering cross sections in the measured spectral region for crystalline and amorphous silicon [14]. The total cross section of RS on

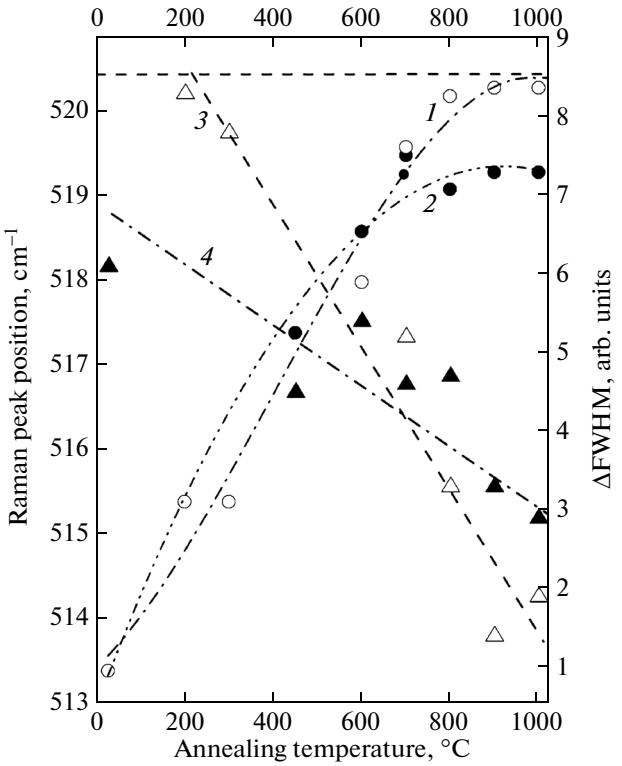

Fig. 3. (*1*, *2*) Peak position of RS on optical phonons and (*3*, *4*) its broadening relative to the peak width in single-crystal silicon for silicon films implanted with hydrogen ions with an energy of 24 keV and a dose of 5×10^{17} cm^{-2} and annealed under pressures of 1 bar and 10.5 kbar as a function of the annealing temperature.

transverse optical phonons is a function of the nanocrystal size D_{nc} (in nm) at $y = 0.1 + \exp(-D_{nc}/25)$. The nanocrystal sizes can be estimated by the frequency shift of the localized optical phonon relative to that in single-crystal silicon, taking into account the error determined by the width of the corresponding peak [15–17]. Estimations show that the size of nanocrystalline inclusions immediately after implantation is ~2 ± 0.5 nm, and their volume fraction is ~1%. After annealing at a temperature of 1000°C, the crystalline-phase fraction reaches ~70%, and the minimum nanocrystal size can be 5.2 nm. The dependence of the crystalline phase fraction on the annealing temperature at atmospheric pressure [6] and under compression of 10.5 kbar is shown in Fig. 4. In this case, the crystallization process can be analyzed using the Avrami formula [18, 19]: $\rho_c = 1 - (1 - \rho_{c0})\exp(-Bt^m)$, where ρ_{c0} is the volume fraction of the crystalline phase in the unannealed films, $B^{1/m} = \nu\exp(-E_a/kT)$, k is the Boltzmann constant, E_a is the crystallization activation energy, t is the annealing time, ν is the frequency factor, an m varies between 3 and 4 [18]. The inset in Fig. 4 shows the dependence of the crystalline-phase fraction on the inverse annealing temperature at atmospheric pressure and a pressure of 10.5 kbar in

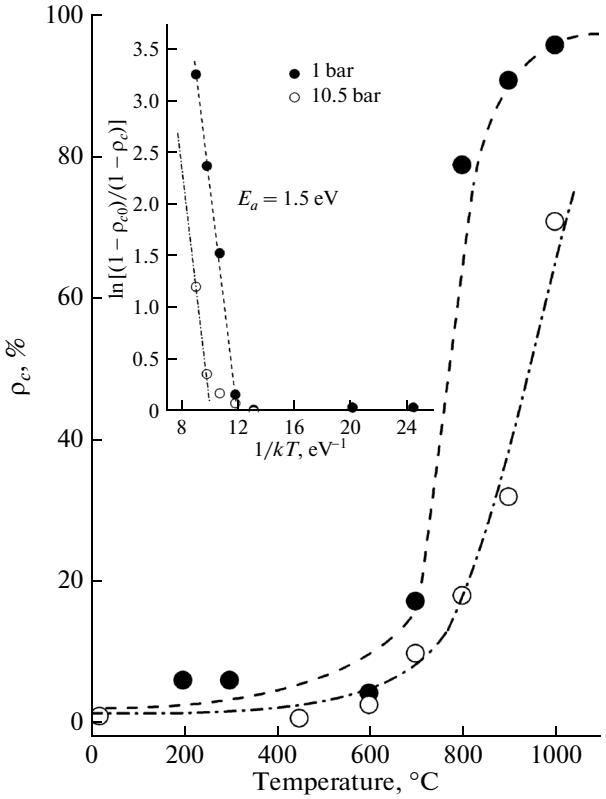

Fig. 4. Volume fraction of the crystalline phase in the silicon layers implanted with hydrogen ions with an energy of 24 keV and a dose of 5×10^{17} cm^{-2} and annealed under pressures of 1 bar and 10.5 kbar as a function of the annealing temperature. The inset shows the logarithmic relative variation of the crystalline phase fraction as a function of the inverse temperature.

$\ln[(1 - \rho_c0)/(1 - \rho_c)]$ and $1/kT$ coordinates. We can see that the dependences in the high-temperature region have the same slope in both cases. This suggests that the crystallization activation energy is independent of hydrostatic compression and is ~1.5 eV in both cases.

The hydrogen state in silicon depends on the presence of structural disorders, traps for H atoms, and the concentration of hydrogen itself. Deep traps in silicon with the level position 1.2–2.0 eV below the hydrogen migration level are as a rule associated with SiH complexes. Their energy levels can be spread because of the high disorientation of Si–Si bonds. In addition to deep levels, there are shallower levels with energies of 0.5–0.7 eV, whose nature is often associated with the formation of interstitial molecular hydrogen. The shallow-level population fraction increases with the hydrogen concentration [20]. The recrystallization of silicon implanted with a high hydrogen-ion dose can be considered a sequence of structural transformations associated with (i) Si–H bond breaking and hydrogen release from traps, (ii) atomic-hydrogen migration to a distance larger than the radius of trapping by a deep center, and (iii) Si–Si bond relaxation. At low annealing temperatures, when the hydrogen concentration is high, ordering results from the relaxation of weakened Si–Si bonds and hydrogen release from shallow levels. In this case, the activation energy of crystalline-phase growth is low and is ~0.1 eV [6]. As the annealing temperature is increased, the hydrogen concentration in the film decreases. This is easily seen from the secondary-ion mass spectrometry data presented in [4, 6]. The decrease in the hydrogen concentration becomes appreciable at temperatures above 500°C at atmospheric pressure and beginning at 700°C at a pressure of ~10^4 bar. Under these conditions, the main limiting process is hydrogen release from deep traps. The activation energy of crystal-matrix ordering increases to ~1.5 eV. An increase in the pressure upon annealing only slows the hydrogen release from the implanted film volume. As in the case of pulsed annealing [6], the activation dependence shifts to higher temperatures. In this case, the activation energy remains almost unchanged, and the effect of high pressures manifest itself in a decrease in the pre-exponential factor which also includes the annealing time and frequency factor. Since the annealing time in the experiments described was constant, we can assume that the increase in the hydrostatic compression is accompanied by a decrease in the frequency factor. Estimations show that the frequency factor decreases by an order of magnitude at a pressure of 10.5 kbar in comparison with its value upon annealing under atmospheric conditions.

4. CONCLUSIONS

The present study showed that crystalline-phase formation under conditions of the annealing of silicon films implanted with hydrogen ions under pressure, as in the case of annealing at atmospheric pressure, occurs with activation energies of ~1.5 eV which corresponds to the diffusion activation energy of atomic hydrogen. An increase in the pressure during annealing leads only to a decrease in the frequency factor, caused by deceleration of the hydrogen release from the implanted film volume.

REFERENCES

1. S. Muchopadhyay, A. Chowdhury, and S. Ray, Thin Solid Films **516**, 6824 (2008).
2. M. N. van den Donker, B. Rech, F. Finger, W. M. M. Kessels, and M. C. M. van de Sanden, Appl. Phys. Lett. **87**, 263503 (2005).
3. N. H. Nickel, N. M. Johnson, and B. Jackson, Appl. Phys. Lett. **62**, 3285 (1993).
4. I. E. Tyschenko, V. P. Popov, A. B. Talochkin, A. K. Gutakovskii, and K. S. Zhuravlev, Semiconductors **38**, 107 (2004).
5. I. E. Tyschenko and V. A. Volodin, Semiconductors **46**, 1286 (2012).

6. I. E. Tyschenko, V. A. Volodin, M. Voelskow, A. G. Cherkov, and V. P. Popov, Semiconductors **47**, 606 (2013).
7. K. Mitani and U. M. Gösele, Appl. Phys. A **54**, 543 (1992).
8. I. E. Tyschenko, K. S. Zhuravlev, A. G. Cherkov, A. Misiuk, and V. P. Popov, Solid State Phenom. **108–109**, 477 (2005).
9. V. Gusakov, Mater. Sci. Semicond. Proc. **9**, 531 (2006).
10. N. H. Nickel and E. A. Schiff, Phys. Rev. B **58** 1114 (1998).
11. D. T. Britton, A. Hempel, M. Harting, G. Kogel, P. Sperr, W. Triftshauser, C. Arendse, and D. Knoesen, Phys. Rev. B **64**, 075403 (2001).
12. Y. Hishikava, J. Appl. Phys. **62**, 3150 (1987).
13. V. Paillard, P. Puech, M. A. Laguna, R. Carles, B. Kohn, and F. Huisken, J. Appl. Phys. **86**, 1921 (1999).
14. E. Bustarret, M. A. Hachicha, and M. Brunel, Appl. Phys. Lett. **52**, 1675 (1988).
15. G. Faraci, S. Gibilisco, P. Russo, and A. Pennisi, Phys. Rev. B **73**, 033307 (2006).
16. J. Zi, H. Buscher, C. Falter, W. Ludwig, K. Zhang, and X. Xie, Appl. Phys. Lett. **69**, 200 (1996).
17. V. A. Volodin and V. A. Sachkov, J. Exp. Theor. Phys. **116**, 87 (2013).
18. J. Gonzalez-Hermandez and R. Tsu, Appl. Phys. Lett. **42**, 90 (1983).
19. T. Okada, T. Iwaki, H. Kasahara, and K. Yamamoto, Solid State Commun. **52**, 363 (1984).
20. B. C. Johnson, J. C. McCallum, A. J. Atanacio, and K. E. Prinee, Appl. Phys. Lett. **85**, 101911 (2009).

Translated by A. Kazantsev